The significant expression of TRPV3 in nasal polyps of eosinophilic chronic rhinosinusitis

Allergology International 66 (2017) 610–616

Contents lists available at ScienceDirect

Allergology International

journal homepage: http://www.elsevier.com/locate/alit

Original article

The significant expression of TRPV3 in nasal polyps of eosinophilic chronic rhinosinusitis

Takahiro Tokunaga [a, b, *], Takahiro Ninomiya [a, b], Yukinori Kato [a], Yoshimasa Imoto [a], Masafumi Sakashita [a], Tetsuji Takabayashi [a], Emiko Noguchi [b], Shigeharu Fujieda [a]

[a] Division of Otorhinolaryngology – Head & Neck Surgery, Department of Sensory and Locomotor Medicine, Faculty of Medical Science, University of Fukui, Fukui, Japan
[b] Department of Medical Genetics, Institute of Basic Medical Sciences, Graduate School of Comprehensive Human Sciences, University of Tsukuba, Ibaraki, Japan

ARTICLE INFO

Article history:
Received 26 August 2016
Received in revised form
2 March 2017
Accepted 15 March 2017
Available online 24 April 2017

Keywords:
Eosinophilic chronic rhinosinusitis
Next-generation sequencing
RNA-seq
TRPV3
Whole-transcriptome analysis

Abbreviations:
CRS, chronic rhinosinusitis; ECRS, eosinophilic CRS; CRSwNP, CRS with nasal polyps; ESS, endoscopic sinus surgery; RNA-seq, RNA sequencing; JESREC study, Japan Epidemiological Survey of Refractory Eosinophilic Chronic Rhinosinusitis study; HPF, high-power field; TRP channel, transient receptor potential channel; TRPV3, TRP cation channel, subfamily V, member 3; FC, fold-change; EGFR, epidermal growth factor receptor; TGF-α, transforming growth factor-α

ABSTRACT

Background: The number of patients with eosinophilic chronic rhinosinusitis (ECRS) has been increasing in recent years in Japan. In ECRS, nasal polyps recur immediately after endoscopic sinus surgery. The molecular biological mechanism underlying the refractoriness of ECRS is unclear.
Methods: Whole-transcriptome analysis with next-generation sequencing (RNA-seq) was conducted to investigate the molecular biological mechanism of ECRS. Real-time PCR, immunohistochemical staining, and immunofluorescence staining were performed to validate the results of RNA-seq.
Results: RNA-seq analysis revealed that in the nasal polyps of ECRS, the levels of 3 transcripts were elevated significantly and those of 7 transcripts were diminished significantly. Among the genes encoding these transcripts, *TRPV3* (transient receptor potential cation channel, subfamily V, member 3) was identified as the only gene that is highly expressed in ECRS nasal polyps but this gene's expression was not previously detected using DNA microarray analysis in peripheral blood eosinophils. *TRPV3* is newly identified here as a gene transcribed in ECRS. Our analysis also revealed that *TRPV3* was highly expressed in the infiltrating eosinophils and mucosal epithelium of the nasal polyps of ECRS, and further that the more severe the refractoriness was after surgery, the higher the *TRPV3* expression was in nasal polyps.
Conclusions: TRPV3 might play a role in the refractoriness of ECRS. Additional studies are required to evaluate the function of TRPV3 in ECRS.

Introduction

Chronic rhinosinusitis (CRS) is a highly common chronic nasal disease, and its symptoms include nasal purulent discharge, nasal congestion, and hyposmia. Several variants of CRS are presented due to diverse underlying cellular and molecular mechanisms, and the phenotypes of CRS are heterogeneous.[1] CRS with nasal polyps (CRSwNP) exhibits more intense eosinophilic infiltration and presence of T-helper type 2 (Th2) cytokines in Western countries than elsewhere; conversely, in East Asia, including in Japan, neutrophil infiltration was previously predominant in CRSwNP.[2] However, in recent years, the number of CRS cases with mucosal eosinophilia has been increasing in Japan with the westernization of eating habits and environments. In eosinophilic cases of CRSwNP, nasal polyps recur immediately after endoscopic sinus surgery

* Corresponding author. Division of Otorhinolaryngology – Head & Neck Surgery, Department of Sensory and Locomotor Medicine, Faculty of Medical Science, University of Fukui, 23-3, Matsuoka-Shimoaizuki, Eiheiji-cho, Yoshida-gun, Fukui 910-1193, Japan.
E-mail address: t-toku3@nifty.com (T. Tokunaga).
Peer review under responsibility of Japanese Society of Allergology.

http://dx.doi.org/10.1016/j.alit.2017.04.002

(ESS). In the Japan Epidemiological Survey of Refractory Eosinophilic Chronic Rhinosinusitis Study (JESREC Study), a multicenter retrospective study, we developed the diagnostic criterion and algorithm for refractory eosinophilic CRS (ECRS). In the study, we specifically noted the relationship between the level of eosinophilia and the refractoriness of CRS: Our work showed that mucosal eosinophilia of ≥70 eosinophils per high-power field (HPF: ×400) was significantly correlated with recurrence after ESS. The factors significantly associated with ECRS recurrence were past history of bronchial asthma, aspirin intolerance, nonsteroidal anti-inflammatory drug intolerance, peripheral blood eosinophilia, and ethmoid-dominant shadow in CT. According to these factors, our algorithm classified CRS into 4 groups: non-ECRS, mild ECRS, moderate ECRS, and severe ECRS. These groups were significantly correlated with the rate of disease recurrence and refractoriness.[3]

Gene expression is an essential factor underlying cellular phenotypes, and a comprehensive catalog of gene transcripts, their structures, and abundance facilitates the elucidation of how gene expression determines phenotypic manifestations. The use of DNA microarrays[4,5] has served as the effective method of choice in gene-expression studies because the microarrays can be used to concurrently probe thousands of transcripts. Although this is a high-throughput approach, it is likely to bias the results because of, for example, the dependency on existing gene models and the potential for cross-hybridization with probes featuring similar sequences. RNA sequencing (RNA-seq) performed using next-generation sequencers is a comparatively new method for analyzing gene expression, and it provides digital readouts for mapping and quantifying transcriptomes.[6,7] In RNA-seq, the following procedure is used: a population of RNA is isolated and transformed into a library of cDNA fragments with adaptors attached, and the cDNA library is then sequenced to obtain short sequences (typically 30–400 nucleotides long) and these short reads are mapped to a reference genome or assembled *de novo*. Subsequently, the expression levels of genes can be determined by counting the number of reads that are aligned to their exons. RNA-seq studies have revealed unknown aspects of transcriptomes, including sequence information on not only exons, but also transcriptional start sites, 5′-untranslated regions, upstream open reading frames, and alternative splicing events.[6,8,9]

Currently, the pathophysiological features of ECRS remain unestablished. Moreover, no reports have been published to date on RNA-seq analysis of ECRS. In this study, we performed RNA-seq analysis of the nasal polyps of CRS in order to reveal the transcripts related to the refractoriness of ECRS. We compared and analyzed the results of RNA-seq and microarray analyses, and then identified and validated the transcripts that exhibited high expression in ECRS.

Methods

Patients of RNA-seq

Nasal polyps were obtained from 10 CRS patients by means of ESS performed at the University of Fukui Hospital, Japan. ECRS was diagnosed based on the JESREC criterion and algorithm, which divided the 10 CRS patients into ECRS and non-ECRS groups.[3] Table 1 and Supplementary Table 1 list the details of the patients' characteristics.

Total RNA isolation and rRNA depletion

Total RNA was isolated from nasal polyps by using an RNeasy® Mini Kit (Qiagen, Hilden, Germany) according to the manufacturer's protocol, and then 4–8 μg of each RNA sample was depleted of rRNA by using a Ribo-Zero™ Gold kit (Epicentre Biotechnologies, Madison, WI, USA) as per manufacturer instructions. RNA was quantified using a NanoDrop1000 spectrophotometer (Thermo Fisher Scientific, Waltham, MA, USA); RNA integrity was evaluated through capillary electrophoresis performed using an Agilent 2100 Bioanalyzer, with RNA 6000 Pico chips (Agilent Technologies, Palo Alto, CA, USA). Only total RNA samples with RNA Integrity Number values[10] of ≥7 were used for the next-generation sequencing analysis.

Table 1
Patient characteristics.

	ECRS	Non-ECRS	*p* value
Number of patients	5	5	
Male/Female	2/3	4/1	n.s.[†]
Age	36 [29–52]	58 [57–59]	0.047*
Number of eosinophils in NP (/HPF)	214.0 [155.0–249.0]	5.0 [5.0–6.0]	0.012*
Peripheral blood eosinophils (%)	13.5 [10.6–13.6]	2.3 [1.8–3.2]	0.008**
JESREC score	15 [15–17]	9 [5–9]	0.010*

Representative values shown as medians with interquartile ranges (in brackets).
*$p < 0.05$, **$p < 0.01$, Wilcoxon rank-sum test.
ECRS, eosinophilic chronic rhinosinusitis; NP, nasal polyps; HPF, high-power field.
[†] χ^2 test.

Library preparation and next-generation sequencing

We used 300–450 ng of rRNA-depleted mRNAs for preparing libraries by using a SOLiD™ Total RNA-Seq Kit (Life Technologies, Grand Island, NY, USA) as per the manufacturer's instructions. The complete library preparation protocol is available at http://tools.invitrogen.com/content/sfs/manuals/cms_078610.pdf. The libraries were subjected to emulsion PCR (SOLiD™ EZ Bead™ Emulsifier kit, Life Technologies) to generate clonal DNA fragments on beads, and this was followed by bead enrichment (SOLiD™ EZ Bead™ Enrichment kit, Life Technologies). Enriched template beads were sequenced on a SOLiD™ 5500xl system (Life Technologies) as single-end, 75-bp reads. Library preparation, fragment-library protocols, emulsion PCR, and all SOLiD-run parameters followed standard Applied Biosystems protocols.

Mapping and processing of sequence data

The obtained sequences were aligned with UCSC human genome 19 (hg19) by using Lifescope™ Genomic Analysis Solutions version 2.5.1 (Life Technologies). Lifescope's default settings were used: 40 alignments per read were allowed, with up to 2 mismatches per alignment.

The resulting aligned reads were analyzed further using Avadis® NGS v1.4.1 (Strand Scientific Intelligence, San Francisco, CA, USA). Avadis NGS assembled the aligned reads into transcripts, either with or without a reference genome (UCSC transcripts), and reported the expression of those transcripts in “Reads Per Kilobase of exon per Million mapped reads,” or RPKM, which is an expression of the relative abundance of transcripts.[6] The *t* test was used to determine differential expression of transcripts in non-ECRS and ECRS samples. The results of multiple tests were corrected using the Benjamini–Hochberg false-discovery rate.[11]

Quantitative real-time RT-PCR (qRT-PCR)

RNA was isolated from nasal polyps obtained from 40 CRS patients except for those of RNA-seq. The polyps were obtained by means of ESS performed at the University of Fukui Hospital, Japan.

ECRS was diagnosed based on the JESREC criterion and algorithm. We performed qRT-PCR by using the TaqMan® Universal Master Mix and Gene Expression Kit (Applied Biosystems, Foster City, CA, USA) according to the manufacturer's instructions. Primer and probe set for TRPV3 (Hs00376854_m1) was purchased from Applied Biosystems.

Immunohistochemical staining

Nasal polyp specimens were collected from 80 CRS patients except for those of RNA-seq. The polyps were obtained by means of ESS performed at the University of Fukui Hospital, Japan. ECRS was diagnosed based on the JESREC criterion and algorithm. The specimens were fixed in neutral buffered formalin (10% (v/v) formalin in water, pH 7.4) and embedded in paraffin wax. Immunohistochemical staining was performed on 4-mm-thick sections by using a TRPV3-specific antibody (Sigma–Aldrich, St. Louis, MO, USA). The number of positive cells of *TRPV3* in the mucosal epithelial cells was counted at HPF (×400) in the three densest areas, and the mean number of positive cells was calculated. Histological examinations were performed unaware of the clinical data. Images from immunofluorescence slides were obtained with an Olympus BX53 inverted research microscope and were collected by using cellSens® Standard software (Olympus, Tokyo, Japan).

Immunofluorescence staining

Nasal polyp specimens were collected from ECRS patients. Peripheral blood was collected from ECRS patients and normal control subjects. The nasal polyp specimens were fixed in neutral buffered formalin (10% (v/v) formalin in water, pH 7.4) and embedded in paraffin wax. Eosinophils were isolated from peripheral blood mononuclear cells by using MACS® Cell Separation system (Miltenyi Biotech, Bergisch Gladbach, Germany) and were cytospinned onto glass slides. To stain TRPV3 and ECP (eosinophil cationic protein), samples were incubated with TRPV3-specific antibody produced in mouse (Sigma–Aldrich) and ECP-specific antibody produced in rabbit (Bioss Antibodies, Woburn, MA, USA) at the dilution mentioned above overnight at 4 °C. After washing with PBS, samples were incubated with Alexa Fluor® 594-conjugated goat anti-mouse IgG (Invitrogen, Carlsbad, CA, USA) and Alexa Fluor® 488-conjugated goat anti-rabbit IgG (Invitrogen) for 1 h at room temperature in the dark. After final washing with PBS, coverslips were mounted onto slides by using SlowFade® Gold Antifade Mountant with DAPI (Thermo Fisher Scientific, Waltham, MA, USA). Images from immunofluorescence slides were obtained with an Olympus BX53 inverted research microscope and were collected by using cellSens® Standard software (Olympus).

Microarray analysis

Microarray assays were performed using the same samples as those used for RNA-seq. We performed microarray assays by using the Illumina BeadArray single-color platform (Illumina, San Diego, CA, USA). In the assay, cRNA was synthesized by using an Illumina TotalPrep RNA Amplification Kit (Ambion, Austin, TX, USA) according to the manufacturer's instructions: 500-ng aliquots of total RNA were reverse-transcribed into first- and second-strand cDNA, and then transcribed to acquire biotin-labeled cRNA. A total of 750 ng of biotin-labeled cRNA was hybridized to each HumanHT-12 v4 Expression BeadChip Kit (Illumina) at 58 °C for 20 h. The hybridized BeadChip was washed and labeled with streptavidin-Cy3 (GE Healthcare, Waukesha, WI, USA) and then scanned with the Illumina BeadStation 500 System (Illumina). We prepared duplicate samples from the same cRNA sample for each BeadChip in order to assess whether the assay performed adequately. The correlation coefficients for replicating RNAs were 0.995–0.998 (r^2).

RNA-seq data were compared with microarray data. All data were $\log_2$-normalized.

Statistical analysis

All data are reported as means ± standard deviation unless otherwise noted. Differences between groups were analyzed by performing one-way ANOVA with Tukey *post hoc* testing or Student's *t* test. Correlations were assessed by using the Pearson correlation. A *p* value or a corrected *p* value ("*q* value") of <0.05 was considered statistically significant. Besides using the statistical tools embedded in Avadis NGS, we performed additional statistical analyses by using R version 2.13.1 for MacOSX GUI 1.40-devel Leopard build 64-bit (R-project, http://www.r-project.org/) and Prism 5.0b for MacOS (MDF, Tokyo, Japan).

Ethical issue

All patients provided informed consent, and the protocol and consent forms governing the procedures for the study were approved by the Research Ethics Committee of the University of Fukui (#20120076).

Results

Alignment results

In the 110 ± 7.1 million-read dataset per sample, 58 ± 8.1% of the reads aligned to the human genome reference hg19. Although <3% of the human genome is composed of exons, 62 ± 2.8% of our uniquely mapped reads overlap gene code exons. These results confirm that our RNA samples are highly enriched for exonic sequences.

Expression analysis

To estimate the expression levels of genes in nasal polyps, we used all of the obtained sequence reads (Fig. 1). A gene's expression level is given by the sum of the RPKM values of its isoforms. The

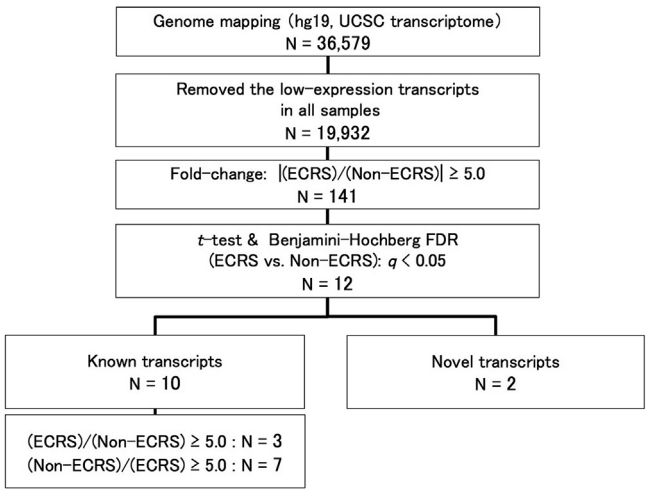

Fig. 1. Flowchart of differential-expression analysis. Differential-expression analysis was performed on the 19,932 transcripts obtained after excluding low-expression transcripts from all samples. Sex-chromosome genes were also excluded from the analysis. Analysis threshold was set as >5-fold. The positive and negative values reflect high and low expression in ECRS, respectively. N, number of transcripts.

distribution of RPKM values was skewed, and the median RPKM values of non-ECRS and ECRS were 33.8 and 32.5, respectively. A total of 36,579 transcripts from the nasal polyps mapped to the reference transcriptome hg19 from UCSC, and 19,932 analyzable transcripts were selected after excluding all of the low-expression transcripts from all samples. Differential-expression analysis was performed on these 19,932 transcripts, and 12 transcripts were found to differ in a statistically significant manner by >5 times between ECRS and non-ECRS. The 12 transcripts included 10 known and 2 previously unidentified transcripts. Details of the transcripts are included in Table 2.

We found that 3 transcripts were expressed at elevated levels in the nasal polyps of ECRS, and among these, the transcript for TRPV3 (transient receptor potential cation channel, subfamily V, member 3) was the only transcript whose expression was not detected in peripheral eosinophils by using microarray analysis.[12]

TRPV3 expression

Real-time PCR and immunohistochemical staining were performed to validate the RNA-seq results: Real-time PCR analysis, performed in 20 non-ECRS cases and 20 ECRS cases, revealed that TRPV3 was expressed at significantly higher levels in the nasal polyp of ECRS than in that of non-ECRS. Expression levels of *TRPV3* mRNA per nanogram of total RNA were 45.2 ± 61.9 copies for non-ECRS and 640.1 ± 819.4 copies for ECRS (Fig. 2A). Moreover, immunohistochemistry were performed in 80 patients: 20 cases of non-ECRS, 20 cases of mild ECRS, 20 cases of moderate ECRS, and 20 cases of severe ECRS. Immunohistochemistry results showed that TRPV3 was highly expressed in the infiltrating cells and mucosal epithelium of the nasal polyps of ECRS (Fig. 2B). To investigate whether the infiltrating TRPV3$^+$ cells are eosinophils or not, immunofluorescence were performed in nasal polyps. Immunofluorescence results showed that ECP was highly expressed in the infiltrating TRPV3$^+$ cells of the nasal polyps of ECRS (Fig. 2C). These results suggest that the infiltrating TRPV3$^+$ cells were eosinophils. Moreover, immunofluorescence staining were performed to investigate whether TRPV3 is expressed in peripheral eosinophils or not. TRPV3 was highly expressed in peripheral eosinophils of both ECRS patients and normal control subjects (Fig. 2D). These results were inconsistent with the result of microarray analysis.[12]

Association between the refractoriness of ECRS and TRPV3 expression

Comparison of the expression in the 4 groups identified using the JESREC algorithm showed that the more severe the refractoriness was, the higher the level of TRPV3 expression was in epithelial cells of nasal polyps. The numbers of positive cells of *TRPV3* expression were 16.2 ± 10.9/HPF for non-ECRS, 33.7 ± 20.6/HPF for mild ECRS, 68.4 ± 29.9/HPF for moderate ECRS, and 52.9 ± 25.2/HPF for severe ECRS (Fig. 3A). Correlation between TRPV$^+$ epithelial cells and infiltrating eosinophils was only a modest, and thus higher level of TRPV3 expression of epithelial cells was independent of an influence of the numbers of infiltrating eosinophils on the refractoriness of ECRS (Fig. 3B).

Table 2
Differentially expressed transcripts.

Gene	Locus	Gene type	Fold-change	*q* value	Eosinophil[†]
High expression in ECRS (Fold-change > 5.0)					
SIGLEC8	chr 19	Protein-coding	7.76	0.047	P
TRPV3	chr 17	Protein-coding	5.81	0.045	A
GPR97	chr 16	Protein-coding	5.56	0.047	P
Low expression in ECRS (Fold-change < −5.0)					
LOC285141	chr 2	Protein-coding	−5.41	0.045	N/A
HABP2	chr 10	Protein-coding	−6.22	0.045	A
CCDC153	chr 11	Protein-coding	−6.59	0.046	N/A
LOC100652764	chr 1	miscRNA	−6.79	0.030	N/A
SCG3	chr 15	Protein-coding	−7.57	0.030	A
LRRC18	chr 10	Protein-coding	−9.98	0.046	A
C1orf129	chr 1	Protein-coding	−11.47	0.030	N/A

P, present; A, absent; N/A, not applicable; ECRS, eosinophilic chronic rhinosinusitis.
[†] Expression profile in peripheral eosinophils determined through microarray analysis by Saito *et al.*[12]

Discussion

In this study, we used next-generation sequencing to perform whole-transcriptome analysis on the nasal polyps of ECRS. This is the first report of a study of this type. We focused on *TRPV3*, the gene specifically expressed in the nasal polyps of ECRS. ECRS is often associated with bronchial asthma. TRPA1 and TRPM8, another subtypes of transient receptor potential (TRP) channel family, may play important roles in the development of bronchial asthma. TRPA1 is expressed in lung fibroblasts,[13] and it is linked to airway inflammation.[14] TRPM8 is expressed in autonomic afferent nerves innervating the broncho-pulmonary system, which may increase airway resistance with neural activation. Activated TRPM8 may be of relevance to aggravation of bronchial asthma.[15] However, there is no report that TRPV3 is expressed in bronchial tissues of asthma. TRPV3 may be a specific molecule in ECRS. TRPV3 has been widely investigated in skin keratinocytes, and Yamamoto-Kasai *et al.* reported that TRPV3 expressed in these cells contributes to the regulation of dendritic cells in atopic dermatitis.[16] However, the function of TRPV3 in the nasal mucous epithelium remains to be clarified.

The TRP channel family represents a group of temperature-sensitive ion channels located on the plasma membrane; these channels contain 6 transmembrane domains and cytosolic N- and C-terminal tails. In recent years, proteins of the TRP channel family, including TRPV1 (capsaicin receptor), have attracted considerable research attention as potential targets for drug development. TRP channels are activated by several chemicals, osmotic stimuli, temperature stimuli, and neuropathic pain, and thus the channels function as transducers that convert environmental information into electronic signals through the flow of cations into the intracellular fluid. Epithelial cells harboring specific activated TRP channels release inflammatory substances such as prostaglandin E2[17] and other cytokines. Furthermore, TRPV3 regulates intracutaneous nitric oxide (NO) synthesis through nitrite reduction independently of NO synthase.[18] A randomized control trial study of CRS patients demonstrated that in patients treated with capsaicin, nasal polyps were significantly smaller than in control patients.[19] These results suggest that the TRP channel family might contribute to inflammation, even if it occurs in the airway.[20]

TRPV3 is located at chromosome 17p13 and is immediately next to *TRPV1*, the gene that encodes the capsaicin receptor. The TRPV3 gene contains 18 exons and encodes a Ca^{2+}-permeable nonselective cation channel that is broadly expressed in skin keratinocytes and oral and nasal mucous epithelia. TRPV3 belongs to the group of warm-sensitive TRP channels whose activation-temperature thresholds range from 31 to 39 °C.[21] Furthermore, several chemical activators for TRPV3 have been identified, and among these, 2-aminoethoxydiphenyl borate, which was first described as an inhibitor of inositol trisphosphate receptors,[22] is the most frequently reported activator.[23,24] Synergism between chemical ligands and temperature and between structurally different chemical ligands is generally observed for thermosensitive TRPV channels; this phenomenon has been described in detail and discussed in a recent review.[25] Other reported TRPV3 activators include camphor,[26,27]

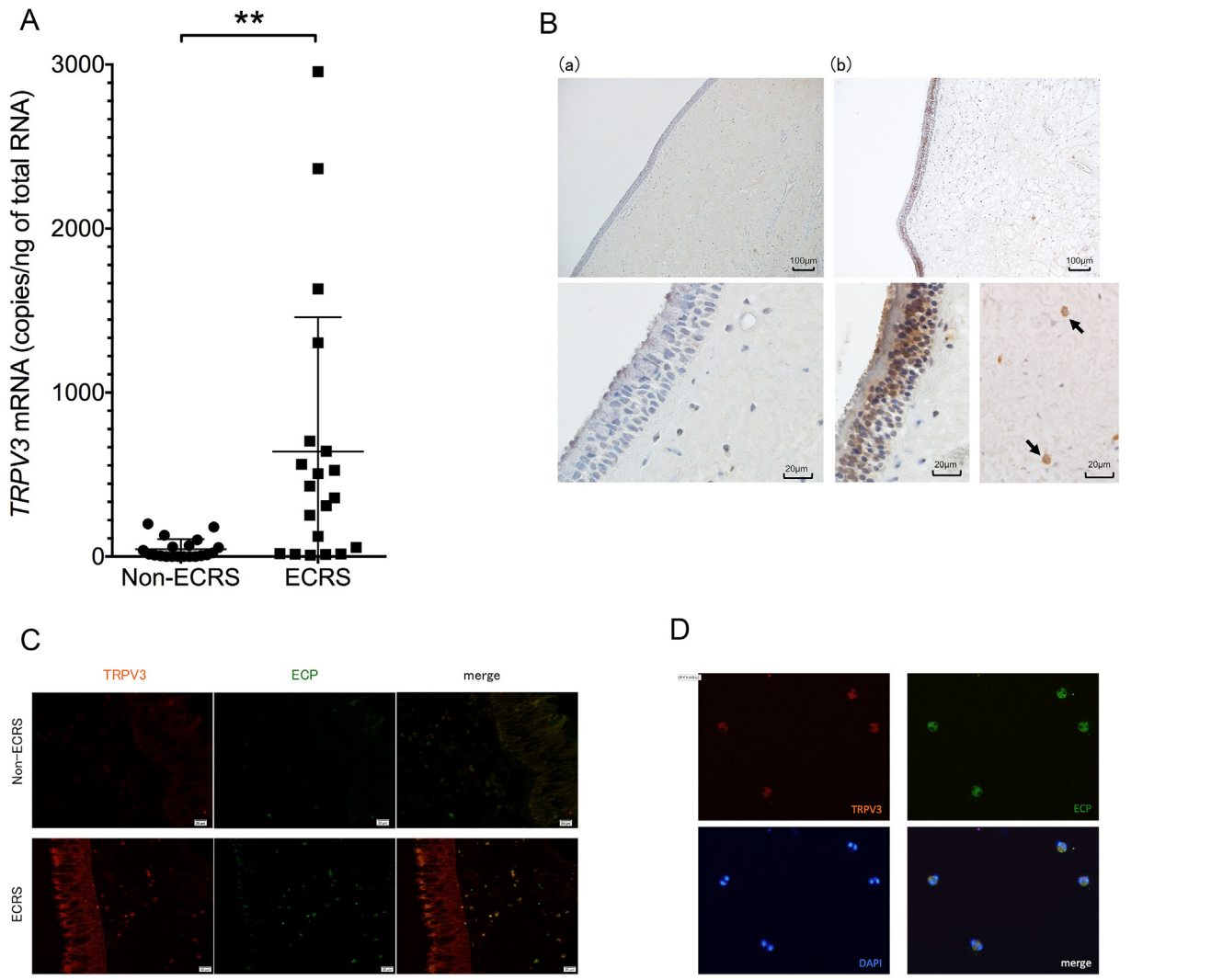

Fig. 2. TRPV3 expression in nasal polyps. **(A)** Total RNA was extracted from the nasal polyps of patients with CRSwNP, and *TRPV3* expression was analyzed using real-time PCR. Lines and error bars represent means and standard deviation. $^{**}p < 0.01$. **(B)** Immunohistochemical staining for TRPV3 in nasal polyps from non-ECRS (a) and ECRS (b). Upper row shows low-magnification (100×). Lower row shows high-magnification (400×). Nasal polyps of ECRS showed more intense TRPV3 staining in epithelial tissues and the infiltrating eosinophils (arrows) than did the polyps of non-ECRS. **(C)** Immunofluorescence staining for TRPV3 and ECP in nasal polyps. Upper row shows non-ECRS. Lower row shows ECRS. Both TRPV3 and ECP were positive in the infiltrating cells of ECRS. **(D)** Immunofluorescence staining for TRPV3 and ECP in peripheral eosinophils of ECRS patients. The same results were obtained with peripheral eosinophils of normal control subjects (figure not shown).

carvacrol, eugenol, thymol,[28] and menthol,[29] which are commonly recognized as flavoring components or skin intensifiers.[30,31] The effect of these components on nasal symptom was examined in several studies. Schriever *et al.* showed that subjective nasal patency of patients with olfactory dysfunction increased with oral menthol application.[32] Whereas these several natural and synthetic materials have been described as TRPV3 activators, the intrinsic activators of TRPV3 remain undefined. However, farnesyl pyrophosphate, an intermediate in the steroid-hormone biosynthesis pathway, has been shown to strongly and specifically activate TRPV3.[33]

TRPV3 regulates diverse functions in skin keratinocyte, including temperature sensing, skin barrier formation, wound healing, hair growth, and itch and pain perceptions.[34] Cheng *et al.* showed that keratinocyte TRPV3 forms a signaling complex with transforming growth factor-α (TGF-α) and epidermal growth factor receptor (EGFR); EGFR activation leads to enhanced TRPV3 channel activity, which in turn stimulates TGF-α release.[35] TGF-α expression in the submucosal tissue was markedly higher in ECRS patients than in non-ECRS patients. Furthermore TGF-α synergized with tumor necrosis factor-α and thereby upregulated mucin 5AC expression in human epithelial cells through the extracellular signal-regulated kinase signaling pathway.[36] If TRPV3 forms a signaling complex with TGF-α/EGFR in the nasal polyps of ECRS, TRPV3 might play a role in mucous hypersecretion, mucous vascularization, and the proliferation of glandular cells and fibroblasts; this might be deeply involved in the recurrence and refractoriness of ECRS. The results of our study indicate that TRPV3 is expressed in the nasal polyps of ECRS but the function of TRPV3 in the nasal polyps remains unknown. Further investigation is required to evaluate the function of TRPV3 in the nasal polyps of ECRS. A TRPV3 antagonist has been created[37] and moved into Phase-II clinical trials for the treatment of neuropathic pain, and additional studies on TRPV3 agonists and antagonists might uncover new therapeutic opportunities for ECRS.

We compared our RNA-seq data with the microarray measurements performed on the same samples. The numbers of transcripts detected by microarray and RNA-seq were 34,692 and 19,932,

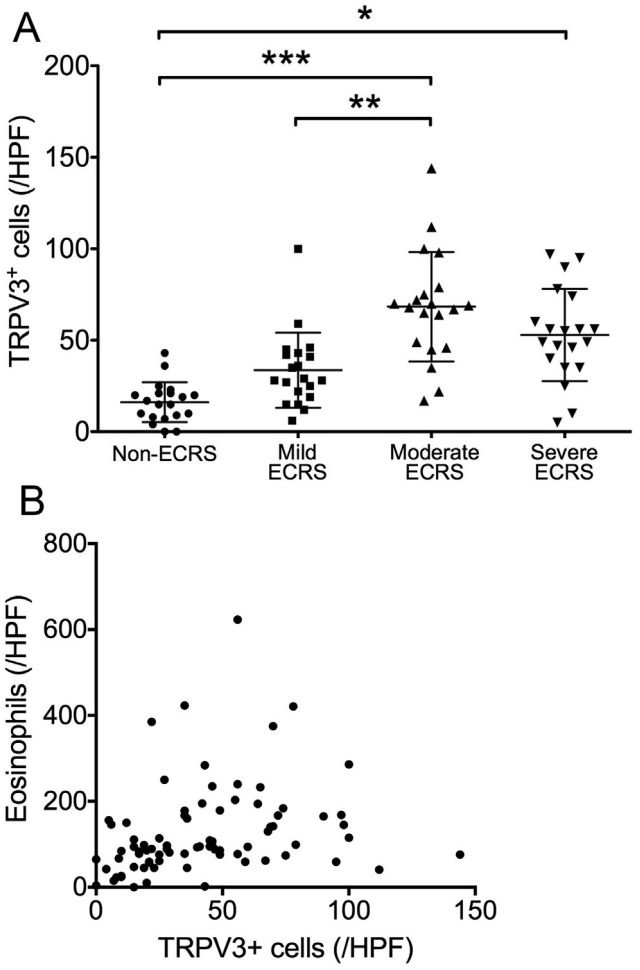

Fig. 3. (A) Number of TRPV3$^+$ cells in nasal polyps from CRSwNP classified by the JESREC algorithm. Lines and error bars represent means and standard deviation. Expression level was correlated with the refractoriness of CRSwNP. Magnification: ×400. $^*p < 0.05$; $^{**}p < 0.01$; $^{***}p < 0.001$. HPF, High-power field. **(B)** Correlation between the number of TRPV3$^+$ epithelial cells and infiltrating eosinophils. Person correlation coefficients: R = 0.27 ($p = 0.017$).

respectively. Among them, the number of transcripts identified by both methods was 16,862. The RNA-seq and microarray results were strongly correlated for gene-expression levels obtained with log-transformed FC values (R = 0.75, $p < 0.001$) (Supplementary Fig. 1), and, furthermore, were comparable to results reported by others (R = 0.67 and 0.80).[38,39] In the case of TRPV3, a significant difference in expression was not detected using microarray analysis, but was confirmed using RNA-seq. Furthermore, real-time PCR and immunofluorescence staining showed high expression of TRPV3 in both nasal polyps and peripheral eosinophils. On the other hand, Saito *et al.* performed the microarray analysis of peripheral eosinophils, which could not detect high expression of TRPV3.[12] They used the GeneChip® Human Genome U133A probe array (Affymetrix, Santa Clara, CA, USA), whereas we used the HumanHT-12 v4 Expression BeadChip Kit (Illumina). Neither of the two arrays could detect high expression of TRPV3. This discrepancy between microarray and RNA-seq may be due to an inappropriate probe hybridized with TRPV3 in microarray kit. Sensitivity of probe is defined by how strongly a probe binds to its target sequence. It affects the strength of the signal read from the microarray.[40]

The rate of concordance between microarray data and RNA-seq data has been investigated in several preceding studies. For instance, Sultan *et al.* measured gene expression difference between two human cell lines (B cells and embryonic kidney cells) and reported that the log-transformed FC values obtained using the two methods significantly correlated (R = 0.88).[41] Wang *et al.*[42] reviewed a comparison of the data from two studies that examined the yeast transcriptome by using microarrays[43] and RNA-seq.[7] Wang *et al.* found that the correlation was very low (R = 0.099–0.177) at low transcript levels in RNA-seq, but comparatively higher (R = 0.509) at moderate transcript levels. This might reflect the narrower dynamic range of microarrays than RNA-seq. Fu *et al.*[38] compared three methods employed for gene expression analysis of human brain samples: use of RNA-seq, microarrays, and mass spectrometry. The correlation coefficient between the microarray data and the RNA-seq data ranged from 0.51 to 0.67, which depend on the type of samples. Moreover, protein abundances quantified using mass spectrometry, which were converted into the equivalent levels of mRNAs, correlated more strongly for the RNA-seq data than for the microarray data. On the other hand, Malone *et al.*[44] showed that high correlations were noted when directly matching microarray intensity values with RNA-seq read counts, although lower correlations were found when matching FC values. A high concordance between RNA-seq data and microarray data was detected in human T cells[39] and in a rat pain model[45] as well. The different strengths of correlations reported by these studies indicate a lack of integrity when assessing the level to which the two methods apply. Here, we report an extent of correspondence between RNA-seq data and microarray data that agrees with the aforementioned reports. The correlation of log-transformed FC values was high.

Acknowledgments

We thank Makiko Imamura and Hiroko Tsuchiya for their excellent assistance. This study was supported by a Grant-in-Aid for Scientific Research (C) (16K11208) and a Grant-in-Aid for Young Scientists (B) (26861360) from the Japan Society for the Promotion of Science, KAKENHI.

This study received the 2015 JSA Best Presentation Award by the Japanese Society of Allergology.

Appendix A. Supplementary data

Supplementary data related to this article can be found at http://dx.doi.org/10.1016/j.alit.2017.04.002.

Conflict of interest

The authors have no conflict of interest to declare.

Authors' contributions

TTo and EN conceived and designed the study. TN and YI collected clinical data. TTo, YK, and YI performed experiments. TTo managed and analyzed the data. TTo, MS, and TTa interpreted the results. TTo, EN, and SF wrote the manuscript. All authors critically read and approved the manuscript.

References

1. Akdis CA, Bachert C, Cingi C, Dykewicz MS, Hellings PW, Naclerio RM, et al. Endotypes and phenotypes of chronic rhinosinusitis: a PRACTALL document of the European Academy of Allergy and Clinical Immunology and the American Academy of Allergy, Asthma & Immunology. *J Allergy Clin Immunol* 2013;**131**:1479–90.
2. Nakayama T, Yoshikawa M, Asaka D, Okushi T, Matsuwaki Y, Otori N, et al. Mucosal eosinophilia and recurrence of nasal polyps – new classification of chronic rhinosinusitis. *Rhinology* 2011;**49**:392–6.
3. Tokunaga T, Sakashita M, Haruna T, Asaka D, Takeno S, Ikeda H, et al. Novel scoring system and algorithm for classifying chronic rhinosinusitis: the JESREC Study. *Allergy* 2015;**70**:995–1003.
4. Fodor SP, Rava RP, Huang XC, Pease AC, Holmes CP, Adams CL. Multiplexed biochemical assays with biological chips. *Nature* 1993;**364**:555–6.

5. DeRisi J, Penland L, Brown PO, Bittner ML, Meltzer PS, Ray M, et al. Use of a cDNA microarray to analyse gene expression patterns in human cancer. *Nat Genet* 1996;**14**:457–60.
6. Mortazavi A, Williams BA, McCue K, Schaeffer L, Wold B. Mapping and quantifying mammalian transcriptomes by RNA-Seq. *Nat Methods* 2008;**5**:621–8.
7. Nagalakshmi U, Wang Z, Waern K, Shou C, Raha D, Gerstein M, et al. The transcriptional landscape of the yeast genome defined by RNA sequencing. *Science* 2008;**320**:1344–9.
8. Cloonan N, Forrest ARR, Kolle G, Gardiner BBA, Faulkner GJ, Brown MK, et al. Stem cell transcriptome profiling via massive-scale mRNA sequencing. *Nat Methods* 2008;**5**:613–9.
9. Pan Q, Shai O, Lee LJ, Frey BJ, Blencowe BJ. Deep surveying of alternative splicing complexity in the human transcriptome by high-throughput sequencing. *Nat Genet* 2008;**40**:1413–5.
10. Schroeder A, Mueller O, Stocker S, Salowsky R, Leiber M, Gassmann M, et al. The RIN: an RNA integrity number for assigning integrity values to RNA measurements. *BMC Mol Biol* 2006;**7**:3.
11. Benjamini Y, Hochberg Y. Controlling the false discovery rate: a practical and powerful approach to multiple testing. *J R Stat Soc Ser B* 2012;**57**:289–300.
12. Saito H, Matsumoto K, Okumura S, Kashiwakura J-I, Oboki K, Yokoi H, et al. Gene expression profiling of human mast cell subtypes: an in silico study. *Allergol Int* 2006;**55**:173–9.
13. Mukhopadhyay I, Gomes P, Aranake S, Shetty M, Karnik P, Damle M, et al. Expression of functional TRPA1 receptor on human lung fibroblast and epithelial cells. *J Recept Signal Transduct Res* 2011;**31**:350–8.
14. Nassini R, Pedretti P, Moretto N, Fusi C, Carnini C, Facchinetti F, et al. Transient receptor potential ankyrin 1 channel localized to non-neuronal airway cells promotes non-neurogenic inflammation. *PLoS One* 2012;**7**:e42454.
15. Xing H, Ling JX, Chen M, Johnson RD, Tominaga M, Wang C-Y, et al. TRPM8 mechanism of autonomic nerve response to cold in respiratory airway. *Mol Pain* 2008;**4**:22.
16. Yamamoto-Kasai E, Yasui K, Shichijo M, Sakata T, Yoshioka T. Impact of TRPV3 on the development of allergic dermatitis as a dendritic cell modulator. *Exp Dermatol* 2013;**22**:820–4.
17. Huang SM, Lee H, Chung M-K, Park U, Yu YY, Bradshaw HB, et al. Overexpressed transient receptor potential vanilloid 3 ion channels in skin keratinocytes modulate pain sensitivity via prostaglandin E2. *J Neurosci* 2008;**28**:13727–37.
18. Miyamoto T, Petrus MJ, Dubin AE, Patapoutian A. TRPV3 regulates nitric oxide synthase-independent nitric oxide synthesis in the skin. *Nat Commun* 2011;**2**:369.
19. Zheng C, Wang Z, Lacroix JS. Effect of intranasal treatment with capsaicin on the recurrence of polyps after polypectomy and ethmoidectomy. *Acta Otolaryngol* 2000;**120**:62–6.
20. Grace MS, Baxter M, Dubuis E, Birrell MA, Belvisi MG. Transient receptor potential (TRP) channels in the airway: role in airway disease. *Br J Pharmacol* 2014;**171**:2593–607.
21. Yao J, Liu B, Qin F. Modular thermal sensors in temperature-gated transient receptor potential (TRP) channels. *Proc Natl Acad Sci U S A* 2011;**108**:11109–14.
22. Maruyama T, Kanaji T, Nakade S, Kanno T, Mikoshiba K. 2APB, 2-aminoethoxydiphenyl borate, a membrane-penetrable modulator of Ins(1,4,5)P3-induced Ca^{2+} release. *J Biochem* 1997;**122**:498–505.
23. Hu H-Z, Gu Q, Wang C, Colton CK, Tang J, Kinoshita-Kawada M, et al. 2-Aminoethoxydiphenyl borate is a common activator of TRPV1, TRPV2, and TRPV3. *J Biol Chem* 2004;**279**:35741–8.
24. Chung M-K, Lee H, Mizuno A, Suzuki M, Caterina MJ. 2-Aminoethoxydiphenyl borate activates and sensitizes the heat-gated ion channel TRPV3. *J Neurosci* 2004;**24**:5177–82.
25. Nilius B, Bíró T, Owsianik G. TRPV3: time to decipher a poorly understood family member! *J Physiol* 2014;**592**:295–304.
26. Moqrich A, Hwang SW, Earley TJ, Petrus MJ, Murray AN, Spencer KSR, et al. Impaired thermosensation in mice lacking TRPV3, a heat and camphor sensor in the skin. *Science* 2005;**307**:1468–72.
27. Xu H, Blair NT, Clapham DE. Camphor activates and strongly desensitizes the transient receptor potential vanilloid subtype 1 channel in a vanilloid-independent mechanism. *J Neurosci* 2005;**25**:8924–37.
28. Xu H, Delling M, Jun JC, Clapham DE. Oregano, thyme and clove-derived flavors and skin sensitizers activate specific TRP channels. *Nat Neurosci* 2006;**9**:628–35.
29. Macpherson LJ, Hwang SW, Miyamoto T, Dubin AE, Patapoutian A, Story GM. More than cool: promiscuous relationships of menthol and other sensory compounds. *Mol Cell Neurosci* 2006;**32**:335–43.
30. Corsini E, Primavera A, Marinovich M, Galli CL. Selective induction of cell-associated interleukin-1alpha in murine keratinocytes by chemical allergens. *Toxicology* 1998;**129**:193–200.
31. Schöll I, Jensen-Jarolim E. Allergenic potency of spices: hot, medium hot, or very hot. *Int Arch Allergy Immunol* 2004;**135**:247–61.
32. Schriever VA, Hummel T. Subjective changes in nasal patency after chewing a menthol-containing gum in patients with olfactory loss. *Acta Otolaryngol* 2015;**135**:254–7.
33. Bang S, Yoo S, Yang T-J, Cho H, Hwang SW. Farnesyl pyrophosphate is a novel pain-producing molecule via specific activation of TRPV3. *J Biol Chem* 2010;**285**:19362–71.
34. Nilius B, Bíró T. TRPV3: a “more than skinny” channel. *Exp Dermatol* 2013;**22**:447–52.
35. Cheng X, Jin J, Hu L, Shen D, Dong X-P, Samie MA, et al. TRP channel regulates EGFR signaling in hair morphogenesis and skin barrier formation. *Cell* 2010;**141**:331–43.
36. Ishinaga H, Shah SA, Sakaida H, Takeuchi K. The role of transforming growth factor-α on mucin overproduction in eosinophilic chronic rhinosinusitis. *Pharmacology* 2011;**88**:302–8.
37. Gomtsyan A, Schmidt RG, Bayburt EK, Gfesser GA, Voight EA, Daanen JF, et al. Synthesis and pharmacology of (pyridin-2-yl)methanol derivatives as novel and selective transient receptor potential vanilloid 3 antagonists. *J Med Chem* 2016;**59**:4926–47.
38. Fu X, Fu N, Guo S, Yan Z, Xu Y, Hu H, et al. Estimating accuracy of RNA-Seq and microarrays with proteomics. *BMC Genomics* 2009;**10**:161.
39. Zhao S, Fung-Leung W-P, Bittner A, Ngo K, Liu X. Comparison of RNA-Seq and microarray in transcriptome profiling of activated T cells. *PLoS One* 2014;**9**:e78644.
40. Lemoine S, Combes F, Le Crom S. An evaluation of custom microarray applications: the oligonucleotide design challenge. *Nucleic Acids Res* 2009;**37**:1726–39.
41. Sultan M, Schulz MH, Richard H, Magen A, Klingenhoff A, Scherf M, et al. A global view of gene activity and alternative splicing by deep sequencing of the human transcriptome. *Science* 2008;**321**:956–60.
42. Wang Z, Gerstein M, Snyder M. RNA-Seq: a revolutionary tool for transcriptomics. *Nat Rev Genet* 2009;**10**:57–63.
43. David L, Huber W, Granovskaia M, Toedling J, Palm CJ, Bofkin L, et al. A high-resolution map of transcription in the yeast genome. *Proc Natl Acad Sci U S A* 2006;**103**:5320–5.
44. Malone JH, Oliver B. Microarrays, deep sequencing and the true measure of the transcriptome. *BMC Biol* 2011;**9**:34.
45. Perkins JR, Antunes-Martins A, Calvo M, Grist J, Rust W, Schmid R, et al. A comparison of RNA-seq and exon arrays for whole genome transcription profiling of the L5 spinal nerve transection model of neuropathic pain in the rat. *Mol Pain* 2014;**10**:7.